Phase Transition Behavior of Unimolecular Micelles with Thermoresponsive Poly(*N*-isopropylacrylamide) Coronas

Shizhong Luo,[‡] Jian Xu,[†] Zhiyuan Zhu,[†] Chi Wu,[‡,§] and Shiyong Liu*[,†,‡]

Department of Polymer Science and Engineering, University of Science and Technology of China, Hefei, Anhui, China, The Hefei National Laboratory for Physical Sciences at Microscale, Hefei, Anhui, China, and Department of Chemistry, The Chinese University of Hong Kong, Shatin, N.T., Hong Kong

Received: February 18, 2006; In Final Form: March 23, 2006

This paper describes the double phase transition behavior of a thermoresponsive poly(*N*-isopropylacrylamide) (PNIPAM) brush at the surface of a hydrophobic core. Reversible addition-fragmentation transfer (RAFT) polymerization of *N*-isopropylacrylamide (NIPAM) was conducted by using a hyperbranched polyester (Boltorn H40) based macroRAFT agent. The resultant multiarm star block copolymer (H40−PNIPAM) exists as unimolecular micelles with hydrophobic H40 as the core, densely grafted PNIPAM brush as the shell. A combination of laser light scattering (LLS) and microdifferential scanning calorimetry (micro-DSC) studies of H40−PNIPAM in aqueous solution reveals double phase transitions of the PNIPAM corona, which is in contrast to the fact that free PNIPAM homopolymer in aqueous solution exhibits a lower critical solution temperature (LCST) at ∼32 °C. The first phase transition takes place in the broad temperature range 20−30 °C, which can be tentatively ascribed to the *n*-cluster-induced collapse of the inner region of the PNIPAM brush close to the H40 core; the second phase transition occurs above 30 °C, which can be ascribed to the outer region of PNIPAM brush. Employing the RAFT chain extension technique, the inner and outer part of PNIPAM brush were then selectively labeled with pyrene derivatives, respectively; temperature-dependent excimer fluorescence measurements further support the conclusion that the inner part of PNIPAM brush collapses first at lower temperatures, followed by the collapse of the outer part at higher temperatures.

Introduction

In aqueous solution, amphiphilic block copolymers can self-assemble into micelles with a hydrophobic block as the core and a hydrophilic block as the shell.[1−3] The microstructure of block copolymer micelles is not static, and there exists dynamic exchange between micelles and unimers, i.e., they tend to be disintegrated upon alteration of external conditions such as concentration, temperature, pH, and ionic strengths, etc.[1,4−6] Chemical cross-linking of the micellar core or shell can lead to micelles with permanent stability.[7−16] When hydrophilic polymer chains are tethered to a hydrophobic multifunctional core, such as dendritic macromolecules and multiarm star block copolymers, they can be considered as unimolecular micelles due to their structural resemblance to amphiphilic block copolymer micelles.[17−28] Moreover, polymeric unimolecular micelles generally possess well-defined chemical structures with predetermined core size, controllable length, and density of grafted chains, thus they could also serve as model systems for block copolymer micelles.

Poly(*N*-isopropylacrylamide) (PNIPAM) is perhaps the most well-known member of the class of thermoresponsive polymers.[29] It undergoes a coil-to-globule phase transition in dilute aqueous solution at its lower critical solution temperature (LCST) of ∼32 °C. PNIPAM grafted to flat or curved surfaces has been explored for a variety of practical applications including controlled drug delivery,[30,31] solute separation,[32] tissue culture substrates,[33,34] and controlling the adsorption of proteins.[35] Application-related properties such as thickness and permeability of PNIPAM layer or shell can be finely tuned with temperature changes.[36] Thus the temperature-dependent conformational changes of PNIPAM chains tethered to flat or curved surfaces have received intensive attention during the past two decades.[36−51]

When polymer chains are tethered by one end to a solid substrate or an interface with a sufficiently high density, the tethered polymer layer falls into the brush regime, i.e., the distance between grafted sites is much less than the size of the polymer coils.[52,53] Polymer chains in the brush are crowded and forced to stretch away from the substrate due to steric exclusion between neighboring chains.

Theoretical predications suggest that the collapse of the surface-tethered polymer brush accompanying a solubility transition proceeds continuously over a much broader range as the solvent quality decreases,[54−57] which is distinct from that of flexible chains free in solution, where the polymer chains adopt random-coil conformations.[58] Experimental results have already confirmed this predication. Balamurugan et al.[37] used surface plasmon resonance (SPR) spectroscopy and contact angle measurements to study a PNIPAM brush grafted from a self-assembled monolayer on bulk gold surface. The SPR results indicated that a PNIPAM brush undergoes a broad transition (over the temperature range 10−40 °C) without abrupt changes; while contact angle measurements, which are more surface sensitive (the outermost 0.5−1 nm) than SPR technique, revealed a sharp change at 32 °C. They proposed that the polymer segments in the outermost region of the brush remain

* To whom correspondence should be addressed. E-mail: sliu@ustc.edu.cn.
† University of Science and Technology of China.
‡ The Hefei National Laboratory for Physical Sciences at Microscale.
§ The Chinese University of Hong Kong.

10.1021/jp061055b CCC: $33.50
Published on Web 04/18/2006

solvated until the LCST, while densely packed segments within the brush layer collapse over a broad range of temperatures.

When PNIPAM chains are tethered to curved surfaces such as latex particles, gold nanoparticles, microgel, and block copolymer micellar cores, the inner part of PNIPAM segments close to the spherical core will be more densely packed than the outer part of PNIPAM segments.[52] Napper et al.[43−45] reported that two phase transitions could be detected for PNIPAM chains adsorbed to the surfaces of latex particles in aqueous solution. The first transition occurred above the θ temperature of PNIPAM (30 °C), which is similar to that of free PNIPAM chains in aqueous solution. The second transition was observed at lower temperatures in the broad range 15−30 °C, which was explained by invoking the *n*-clusters concept of de Gennes.[57,59] According to this concept, it is possible for certain types of polymer chains to exhibit attractive *n*-body ($n > 2$) interactions, while the two-body interactions are still repulsive. The attractive *n*-body interactions can lead to *n*-clusters, which can induce the collapse of polymer brush. When the polymer brush is grafted at a spherical surface, the densely grafted inner layer has a larger possibility to exhibit *n*-clustering-induced collapse, as compared to the outer part of the brush.[57,59]

For PNIPAM chains tethered to gold nanoparticles, Tenhu et al.[42] also reported two phase transitions by microcalorimetry. They ascribed the phase transition at ∼32 °C to that of the inner part of PNIPAM segments, while the phase transition at ∼40 °C was ascribed to that of the outer part of PNIPAM segments. We also noticed that, when PNIPAM chains are tethered to a microgel[49,60] or a micellar core,[41] temperature-dependent laser light scattering (LLS) studies typically reveal that the size of grafted PNIPAM brush exhibits a gradual decrease in the temperature range 20−30 °C, followed by a relatively sharp decrease around ∼32 °C.

It should be noted that, in the studies of Napper et al.,[43−45] PNIPAM is sterically tethered to PS latex particles, additional adsorption of other parts of the PNIPAM chain may take place except for the chain end at increasing temperatures; further adsorption of free PNIPAM chains in the solution is also highly possible. Au−S bonds linking PNIPAM chains to gold nanoparticles may not be stable enough at elevated temperatures.[42] In the case of block copolymer micelles,[41] the critical micellization concentration (cmc) will change with temperature; this will lead to further incorporation of unimer chains into the micelles. In all of the above cases, temperature-dependent LLS or microcalorimetry results are therefore complicated to interpret due to interference from additional adsorption/aggregation upon temperature increase.

To study the phase transition behavior of the PNIPAM corona of unimolecular micelles will be more straightforward and convincing because the length, size, and density of grafted PNIPAM chains are predetermined.[23,61] Herein we prepared unimolecular core−shell nanostructures with a PNIPAM corona based on commercially available fourth-generation hyperbranched polyester (Boltorn H40) via the RAFT technique. Boltorn H40 as an ideal dendrimer would theoretically have 64 primary hydroxyl groups (Scheme 1).[62−67] The molecular size of fractionated Boltorn H40 (denoted as H40) is estimated to be ca. 3 nm,[63,66,67] thus the RAFT grafting of *N*-isopropylacrylamide (NIPAM) from an H40 core results in a densely packed PNIPAM brush surrounding the hydrophobic H40 core. The thermoresponsive phase transition behavior of PNIPAM brush is characterized in detail by dynamic and static laser light scattering (LLS), microdifferential scanning calorimetry (micro-DSC), and excimer fluorescence techniques. We demonstrate here that PNIPAM brush at the surface of the hydrophobic H40 core exhibits double thermal phase transition behavior.

SCHEME 1: (a) Idealized Molecular Structure of H40; (b) the Chemical Structure of H40−PNIPAM

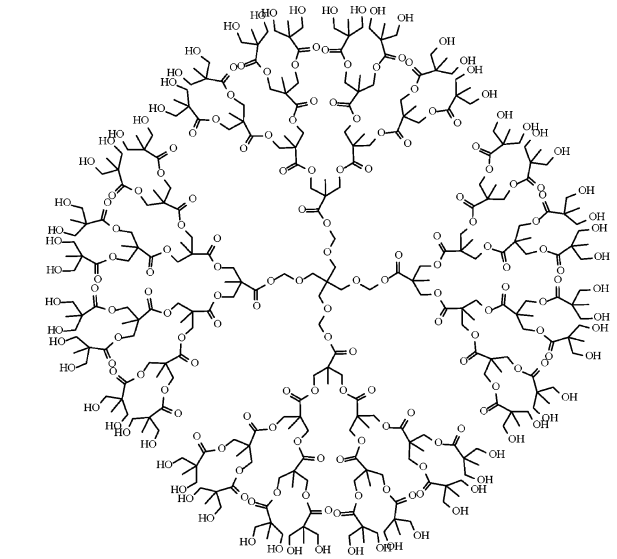

Experimental Section

Materials. Hyperbranched polyester Boltorn H40 was obtained from Perstorp Polyols AB. It was further fractionated with a typical 20% yield by using a procedure reported by Tsukruk et al.[62−64] Boltorn H40 as an ideal dendrimer would theoretically have 64 primary hydroxyl groups and a molar mass of 7316 g mol^{-1} (Scheme 1). SEC analysis of fractionated Boltorn H40 indicates a $M_n \sim 6500$ g mol^{-1} and a polydispersity of 1.40.[68] We denote the fractionated hyperbranched polyester as H40 here. According to Tsukruk et al.,[63] the degree of branching of H40 was 0.4 and the average number of monomeric units (the degree of polymerization) was ca. 60. *N*-isopropylacrylamide (NIPAM) was purified by recrystallization in a benzene/*n*-hexane mixture. THF was distilled over sodium/benzophenone. (4-(1-Pyrenyl)butyl) acrylate (PyBA) and an H40-based macroRAFT agent were synthesized according to previously reported procedures.[68]

Sample Preparation. *Synthesis of H40−PNIPAM.*[68] The general procedure for synthesizing H40−PNIPAM was as follows. A glass ampule was charged with H40 macroRAFT agent, AIBN, and NIPAM in THF; it was then degassed by three freeze−thaw cycles and sealed under vacuum. The polymerization was carried out at 80 °C for 12 h. The mixture was precipitated into anhydrous diethyl ether twice. The product was collected by filtration and then dried in a vacuum oven at room temperature. The chemical structure of H40−PNIPAM was shown in Scheme 1.

Synthesis of Pyrene-Labeled H40−PNIPAM. Pyrene-labeled multiarm star block copolymer, H40−PNIPAM(Py), was synthesized by RAFT copolymerization of NIPAM and PyBA (1.5 mol %) by using an H40 macroRAFT agent according to a similar procedure used to synthesize H40−PNIPAM. By employing the RAFT chain extension technique, H40−PNIPAM-(Py)-*b*-PNIPAM and H40−PNIPAM-*b*-PNIPAM(Py) are also synthesized, with the inner and outer part of the PNIPAM brush labeled with pyrene derivatives, respectively.

Cleavage of Grafted PNIPAM Chains.[69] 0.5 g of H40−PNIPAM (0.5 g) or H40−PNIPAM(Py) (0.5 g) was dissolved in 100 mL of anhydrous THF, and excess lithium chloride and potassium borohydride were slowly added to the solution. The reaction was refluxed with vigorous stirring under nitrogen until the evolution of gas ceased. After the solvent was removed under reduced pressure, the residue was dissolved in methylene chloride and an equal volume of water added. This mixture was extracted three times with methylene chloride, and the organic layers were collected and combined. After concentrating the solution, it was then precipitated in diethyl ether for 3 times. The cleaved thiol-end-functionalized PNIPAM[42] was dried in a vacuum oven overnight at room temperature. The above reduction procedure degraded the hyperbranched polyester core and recovered the grafted PNIPAM for further SEC characterization.

Characterization. *Nuclear Magnetic Resonance (NMR) Spectroscopy.* All ^{1}H NMR spectra were recorded using a Bruker 300 MHz spectrometer. H40- and H40-based macroRAFT agents were analyzed in *d*-DMSO, and H40−PNIPAM and H40−PNIPAM(Py) were analyzed in *d*-DMSO or $CDCl_3$.

Size Exclusion Chromatography (SEC). Molecular weight distributions were determined by SEC using a series of three linear Styragel columns, HT3, HT4, and HT5, and an oven temperature of 60 °C. A Waters 1515 pump and a Waters 2414 differential refractive index detector (set at 30 °C) were used. The eluent was DMF + 1 g/L LIBr at a flow rate of 1.0 mL/min. Polystyrene standards were used for calibration.

Laser Light Scattering (LLS). A commercial spectrometer (ALV/DLS/SLS-5022F) equipped with a multi-tau digital time correlator (ALV5000) and a cylindrical 22 mW UNIPHASE He−Ne laser ($\lambda_0 = 632$ nm) as the light source was used. In static LLS, we can obtain the weight-average molar mass (M_w) and the *z*-average root-mean-square radius of gyration ($\langle R_g^2\rangle^{1/2}$ or written as $\langle R_g\rangle$) of polymer chains in a dilute solution from the angular dependence of the excess absolute scattering intensity, known as the Rayleigh ratio $R_{vv}(q)$, as

$$\frac{KC}{R_{vv}(q)} \approx \frac{1}{M_w}\left(1 + \frac{1}{3}\langle R_g^2\rangle q^2\right) + 2A_2 \qquad (1)$$

where $K = 4\pi^2 n^2 (dn/dC)^2/(N_A\lambda_0^4)$ and $q = (4\pi n/\lambda_0)\sin(\theta/2)$ with N_A, dn/dC, n, and λ_0 being the Avogadro number, the specific refractive index increment, the solvent refractive index, and the wavelength of the laser light in a vacuum, respectively; A_2 is the second virial coefficient. Strictly speaking, here $R_{vv}(q)$ should be $R_{vu}(q)$ because there is no analyzer before the detector. However, the depolarized scattering of the solution studied is insignificant so that $R_{vu}(q) \sim R_{vv}(q)$. Also note that, in this study, the sample solution for LLS was so dilute (1.0×10^{-6} g/mL) that the extrapolation of $C \rightarrow 0$ was not necessary, and the term $2A_2C$ in eq 1 can be neglected; the obtained M_w value is denoted as the apparent molecular weight, $M_{w,app}$.

The specific refractive index increment, dn/dC, was determined by a precise differential refractometer at 632 nm.[70] For PNIPAM homopolymer in water, dn/dC values exhibit weak temperature dependence, which were 0.167 and 0.174 mL/g at 25 and 40 °C, respectively.[71] dn/dC of H40−PNIPAM in water was determined to be 0.154 mL/g at 15 °C. The same dn/dC value of 0.154 mL/g was used for pyrene-labeled H40−PNIPAM, assuming that the incorporation of 1.5 mol % pyrene monomer units into the PNIPAM chain has a negligible effect on dn/dC. The above dn/dC values are then used in the determination of $M_{w,app}$ of H40−PNIPAM, H40−PNIPAM(Py), H40−PNIPAM(Py)-*b*-PNIPAM, and H40−PNIPAM-*b*-PNIPAM-(Py).

In dynamic LLS, the Laplace inversion of each measured intensity−intensity time correlation function $G^{(2)}(q,t)$ in the self-beating mode can lead to a line-width distribution $G(\Gamma)$. For a pure diffusive relaxation, Γ is related to the translational diffusion coefficient D by $(\Gamma/q^2)_{C\rightarrow 0, q\rightarrow 0} \rightarrow D$, or further to the hydrodynamic radius R_h via the Stokes−Einstein equation, $R_h = (k_B T/6\pi\eta_0)/D$, where k_B, T, and η_0 are the Boltzmann constant, the absolute temperature, and the solvent viscosity, respectively.

Microdifferential Scanning Calorimetry (Micro-DSC). The copolymer solutions were measured by a VP-DSC microcalorimeter (MicroCal Inc) at an external pressure of 180 kPa. The cell volume was 0.157 mL. The heating rate was 1.0 °C/min, and the instrument response time was set at 5.6 s. All the micro-DSC data were corrected for instrument response time and analyzed using the software in the calorimeter.

Fluorescence Measurements. Fluorescence spectra were recorded using a JASCO FP-6200 spectrofluoriometer. The temperature of the water-jacketed cell holder was controlled by a programmable circulation bath. The slit widths were set at 5 nm for both the excitation and the emission. In a 1-cm cell, the samples were heated slowly with the heating rate of 0.1 °C/min. The excimer-to-monomer ratio was calculated as the ratio of the emission intensity at 480 nm to that of the emission at 373 nm.

Results and Discussion

Syntheses of H40-PNIPAM and Pyrene-Labeled H40-PNIPAM. The syntheses of H40−PNIPAM and pyrene-labeled H40−PNIPAM followed previously reported procedures.[68] SEC analysis in DMF of H40−PNIPAM gives a symmetric elution peak with a number-average molecular weight (M_n) of 4.75×10^5 g mol^{-1} and a polydispersity of 1.22, while H40 itself has a $M_n = 6500$ g mol^{-1} and polydispersity of 1.40. The relatively narrow polydispersity of H40−PNIPAM suggested the controlled RAFT polymerization of NIPAM using an H40 macroRAFT agent. Because SEC analysis uses linear polystyrene as standards and H40−PNIPAM take a dendritic conformation, static LLS was used to determine the absolute molecular weight of H40−PNIPAM. The apparent weight-average molecular weight ($M_{w,app}$) determined by LLS in water was 6.9×10^5 g mol^{-1}.

To determine the actual molecular weight of the PNIPAM arm and grafting density, PNIPAM was cleaved from H40−PNIPAM through reduction and purification, SEC analysis of the recovered PNIPAM revealed a M_n of 1.10×10^4 g mol^{-1} and a polydispersity of 1.20, and the degree of polymerization (DP) of PNIPAM arm was then calculated to be ~97. Considering that the $M_{w,app}$ of H40−PNIPAM is 6.9×10^5 g mol^{-1}, and the weight-average molar mass (M_w) of grafted PNIPAM chain is 1.32×10^4 g mol^{-1}, the number of PNIPAM arms grafted per H40 core is calculated to be ~52. There are about 60 hydroxyl groups on the surface of H40,[62−64] so ca. 90% of the surface-functionalized RAFT groups participated in the polymerization, assuming 100% functionalization of H40 during

TABLE 1: Molecular Parameters of H40−PNIPAM and Pyrene-Labeled H40−PNIPAM

	M_n g mol^{-1}[a]	M_w/M_n[a]	$M_{w,app}$ g mol^{-1}[b]	$M_{n,PNIPAM}$ g mol^{-1}[c]	M_w/M_n[c]	DP of PNIPAM	number of arms[d]
H40−PNIPAM	4.75×10^5	1.22	6.9×10^5	1.10×10^4	1.20	97	52
H40−PNIPAM(Py)	5.23×10^5	1.25	8.6×10^5	1.36×10^4	1.16	120	54
H40−PNIPAM(Py)-*b*-PNIPAM	5.05×10^5	1.31	7.1×10^5	/	/	53/66[e]	/
H40−PNIPAM-*b*-PNIPAM(Py)	4.90×10^5	1.28	7.5×10^5	/	/	67/59[e]	/

[a] Determined by SEC using DMF + 1.0 g/L LIBr as eluent. [b] Determined in water by static LLS at 15 °C. [c] Determined by SEC after cleavage via reduction with KBH_4. [d] Calculated from $M_{w,app}$ determined by LLS and molecular weight of cleaved PNIPAM arms determined by SEC. [e] Degree of polymerization of the inner block and outer block determined by static LLS for the precursor and final dendritic macromolecules, assuming the number of grafted chain per H40 core is 52.

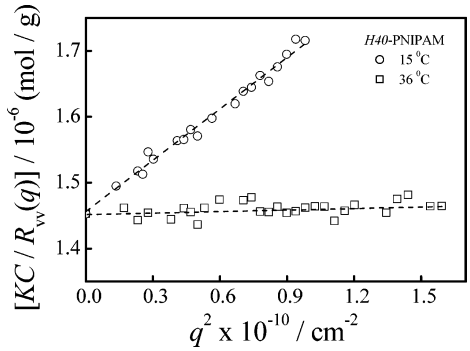

Figure 1. Scattering vector (q) dependence of Rayleigh ratio $R_{vv}(q)$ of H40−PNIPAM in aqueous solution at two different temperatures, where the concentration is 1.0×10^{-6} g/mL.

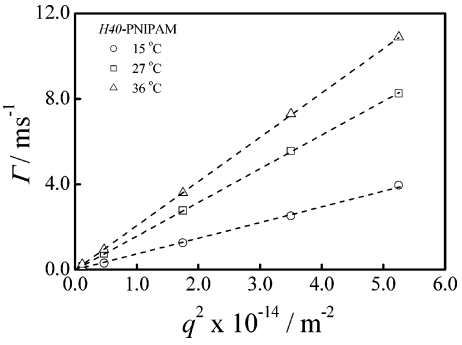

Figure 2. Scattering vector (q) dependence of the average characteristic line width (Γ) of H40−PNIPAM in aqueous solution at different temperatures, where the concentration is 1.0×10^{-6} g/mL.

preparation of the macroRAFT agent.[68] H40−PNIPAM(Py) was characterized in similar procedures and the results are shown in Table 1. For H40−PNIPAM(Py)-*b*-PNIPAM and H40−PNIPAM-*b*-PNIPAM(Py), cleavage of the grafted and partially labeled PNIPAM chains was not conducted, and the DP of the pyrene-labeled and unlabeled block is calculated on the static LLS results, assuming that the number of grafted chain per H40 core is ∼52. The pyrene content relative to the PNIPAM block determined by UV−vis absorption using 1-pyrenebutanol as a model compound is ca. 1.3 mol %. The molecular parameters of H40−PNIPAM and pyrene-labeled H40−PNIPAM are summarized in Table 1.

LLS Characterization. LLS was used to characterize the chain conformational changes of H40−PNIPAM in aqueous solution upon heating. It is well-known that PNIPAM homopolymer undergoes a coil-to-globule phase transition in dilute aqueous solution at its LCST of ca. 32 °C.[29] At a temperature below the LCST, PNIPAM chains adopt a randomly coiled structure due to the predominantly intermolecular hydrogen bonding between PNIPAM chains and water molecules. At a temperature above the LCST, intramolecular hydrogen-bonding interactions between C═O and N−H groups renders the chains to become compact and collapse, reducing their water solubility.

From a structural point of view, dendritic H40−PNIPAM in aqueous solution will exist as unimolecular micelles with H40 as the core and PNIPAM as the shell at low temperatures. The molecular size of H40 core was estimated to be ca. 3 nm,[63,66,67] the number of grafted PNIPAM chains per H40 core were ∼52, thus the grafting density at the surface of H40 core surface was calculated to be 0.46 nm^2 per PNIPAM chain. Compared to the hydrodynamic diameter of free PNIPAM chain with a DP of 97 (around 5 nm), the grafting of PNIPAM resulted in a densely packed PNIPAM brush surrounding the hydrophobic core.

Figure 1 shows typical angular dependences of the Rayleigh ratio $[KC/R_{vv}(q)]$ of H40−PNIPAM at 15 °C and 36 °C, which is below and above the LCST of free PNIPAM chains in water. The concentration for LLS studies is chosen to be very low (1.0×10^{-6} g/mL) to avoid any possible aggregation between dendritic H40−PNIPAM above the phase transition. It can be clearly seen that the slope in Figure 1 decreases with increasing temperature. On the basis of eq 1, this reflects the decrease of $\langle R_g \rangle$, i.e., the shrinking (or collapse) of the grafted PNIPAM brush at higher temperatures. The extrapolation of $KC/R_{vv}(q)$ to $q \rightarrow 0$ at two different temperatures leads to almost the same intercept (±5%), indicating that $M_{w,app}$ is nearly constant in the temperature range 15−36 °C. $M_{w,app}$ was determined to be 6.9×10^5 g mol^{-1}. We then further investigated the dendritic macromolecules at a higher concentration of 1.0×10^{-3} g/mL, scattering intensity remained constant below 30 °C and showed 10−15% increase in the temperature range 30−40 °C. This indicates that partial aggregation between dendritic macromolecules takes place above the LCST of PNIPAM shell.

Figure 2 shows the q^2 dependence of the average characteristic line width (Γ) of H40−PNIPAM in water at different temperatures, where the concentration is 1.0×10^{-6} g/mL. It reveals that Γ is a linear function of q^2 and the extrapolation of Γ to $q \rightarrow 0$ passes through the origin, confirming that the apparent diffusion coefficient depends only on the translational motion during heating. Here, the slope of Γ vs q^2 leads to the translational diffusion coefficient D and further to the hydrodynamic radius R_h by the Stokes−Einstein equation, $R_h = (k_B T/6\pi\eta_0)/D$.

Figure 3 shows typical plots of the hydrodynamic radius distribution $f(R_h)$ of H40−PNIPAM at three different temperatures: 15, 27, and 36 °C. It can be clearly seen that the distribution curve shifts to the left with increasing temperatures. The average hydrodynamic radius ($\langle R_h \rangle$) of H40−PNIPAM at 15, 27, and 36 °C are 26, 16, and 14 nm, respectively. This should be ascribed to the collapsing of the PNIPAM brush. Unimolecular micelles at different temperatures are relatively monodisperse, and the polydispersity indexes of the size distributions (μ_2/Γ^2) are typically less than 0.12. μ_2/Γ^2 is relatively smaller at 36 °C ($\mu_2/\Gamma^2 = 0.08$) than that at 15 °C ($\mu_2/\Gamma^2 = 0.12$) and 27 °C ($\mu_2/\Gamma^2 = 0.11$).

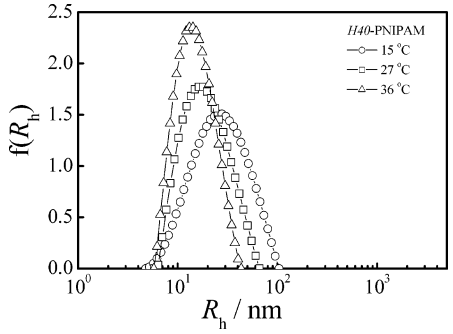

Figure 3. Typical hydrodynamic radius distributions, $f(R_h)$, of H40−PNIPAM-Py aqueous solution at different temperatures, where the concentration is 1.0×10^{-6} g/mL.

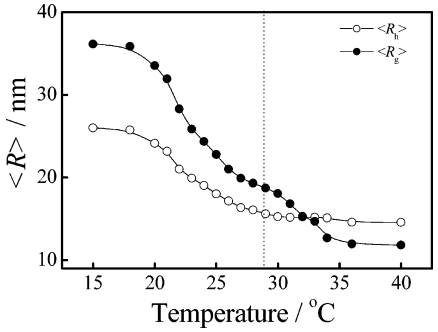

Figure 4. Temperature dependences of the average radius of gyration, $\langle R_g \rangle$, and average hydrodynamic radius, $\langle R_h \rangle$, of H40−PNIPAM in water during the heating process, where the concentration of H40−PNIPAM is 1.0×10^{-6} g/mL.

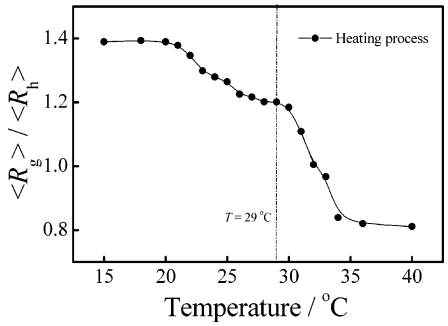

Figure 5. Temperature dependences of $\langle R_g \rangle / \langle R_h \rangle$ for aqueous solution of H40−PNIPAM during the heating process.

The grafting density of PNIPAM chains at the hydrophobic H40 core surface is very high, ca. 0.46 nm^2 per chain. PNIPAM chains in the brush are expected to be crowded and forced to stretch away from the substrate to avoid overlapping. Theoretical predictions suggest that strong interchain repulsions are present in the brush and should cause a broadening of the transition of polymer chains.[54−57] Considering the molecular size of H40 core (3 nm in diameter) and $\langle R_h \rangle$ of H40−PNIPAM in the swollen state at 15 °C (26 nm), the average length of a surface-attached PNIPAM chain with a DP of 97 is about 24.5 nm. In preliminary experiments, we found that the $\langle R_h \rangle$ of free PNIPAM chains with a DP of ∼100 in water is about 2.5 nm, i.e., the dimensions of free PNIPAM chains are ∼5 nm. So the dimension of PNIPAM chains in the brush is much larger than that of the free PNIPAM chains with the same DP in solution (∼5 nm). This indicates that the surface-attached PNIPAM chains are highly extended due to steric exclusions imposed by neighboring chains in the brush. The dynamic LLS results agree favorably with those obtained from PNIPAM- and PS-stabilized gold or latex nanoparticles, where chain stretching was observed.[42,45]

It should be noted that, in the above calculation, the molecular size of the H40 core is fixed at 3 nm. Theoretically, the dimension of the H40 core is expected to expand to some extent due to the dense grafting of PNIPAM chains. Tsukruk et al.[72−75] recently studied the interfacial behavior of hyperbranched polyesters with different generations. They found that H40 possesses dense, compact, and globular molecular structure, which is usually observed only for high-molecular-weight dendrimers. In combination with their observations and the fact that PNIPAM brush was tethered to the hydrophobic H40 core, the size change of the hyperbranched core after PNIPAM grafting was neglected for simplicity.

The issue most interesting to us is the collapsing process of the PNIPAM brush with increasing temperatures. Figure 4 shows typical temperature dependences of average radius of gyration ($\langle R_g \rangle$) and average hydrodynamic radius ($\langle R_h \rangle$) of H40−PNIPAM in water upon increasing temperatures. Each data point was obtained after the measured values were stable.

Upon heating, $\langle R_h \rangle$ decreased monotonically from 26 to 14 nm in the temperature range 15−40 °C. This corresponds to ca. 85% shrinkage of the hydrodynamic volume of the PNIPAM brush at elevated temperatures. The transition is relatively broad, spanning about 15 °C. It is well-known that, for PNIPAM homopolymer chains, $\langle R_h \rangle$ drops abruptly in the narrow temperature range 30−33 °C.[29] The more fascinating thing is the temperature dependences of $\langle R_g \rangle$ (Figure 4). It clearly reveals that the PNIPAM brush undergoes a two-stage collapse. The $\langle R_g \rangle$ is about 36 nm at 15 °C, and it gradually decreases to 19 nm at 29 °C. Above 29 °C, $\langle R_g \rangle$ further decreases from 19 to 12 nm in the temperature range 29−36 °C.

The two-stage collapse behavior hints at the double phase transition behavior of a PNIPAM brush; this observation is qualitatively in agreement with results obtained by Tenhu et al.[42] and Napper et al.[44,45] for a PNIPAM brush tethered to gold nanoparticles or latex particles. The inner and outer part of a PNIPAM brush has different extent of chain crowding due to decreasing chain density from being close to the core to the outer part of the corona. The inner part of the PNIPAM brush are more densely packed and crowded. Although we observed two phase transitions by LLS, currently we cannot ascribe the first transition at lower temperatures to the inner part of brush. This question will be solved through excimer fluorescence studies of pyrene-labeled samples, which are described later.

It is well-known that the ratio of $\langle R_g \rangle / \langle R_h \rangle$ reflects the conformation of a polymer chain or the density distribution of chain segments in core−shell nanoparticles. A smaller $\langle R_g \rangle / \langle R_h \rangle$ value typically hints at a higher chain segment density. For example, for linear and flexible polymer chains, $\langle R_g \rangle / \langle R_h \rangle$ is around 1.5, but for a uniform nondraining sphere, $\langle R_g \rangle / \langle R_h \rangle$ drops to 0.774. A ratio of 0.8−1.5 is found for hyperbranched or dendritic macromolecules.[58] Figure 5 shows the typical temperature dependences of $\langle R_g \rangle / \langle R_h \rangle$ of H40−PNIPAM in water during the heating process. It again clearly exhibits a two-stage collapse of the PNIPAM brush. $\langle R_g \rangle / \langle R_h \rangle$ gradually decreases from 1.38 to 1.20 when the temperature increases from 15 to 29 °C; $\langle R_g \rangle / \langle R_h \rangle$ then exhibits further decrease from 1.20 to 0.82 in the range 29−36 °C. At temperatures higher than 36 °C, $\langle R_g \rangle / \langle R_h \rangle$ is nearly independent of temperature, indicating that the PNIPAM brush reaches the finally collapsed state.

We have also studied the variation of $\langle R_g \rangle$, $\langle R_h \rangle$, and $\langle R_g \rangle / \langle R_h \rangle$ with temperatures during the cooling process. The collapsing and reswelling of a PNIPAM brush of H40−PNIPAM upon heating and cooling are generally reversible, with more gradual changes occurring in the cooling cycle. We can also observe the two-stage re-swelling of PNIPAM brush during the cooling

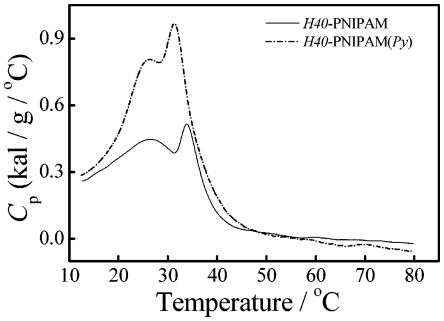

Figure 6. Temperature dependence of partial heat capacity, C_p, of aqueous solutions of H40−PNIPAM and H40−PNIPAM(Py) at a concentration of 1.0×10^{-3} g/mL, the heating rate is 1.0 °C/min.

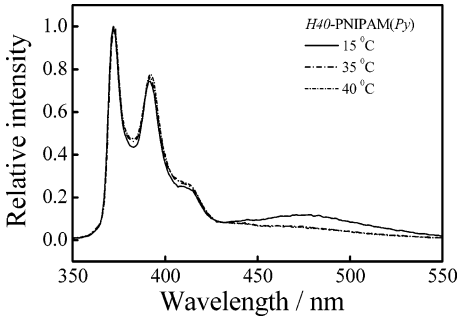

Figure 7. Normalized fluorescence emission spectra at different temperatures for aqueous solution of H40−PNIPAM(Py). The polymer concentration is 1.0×10^{-3} g/mL.

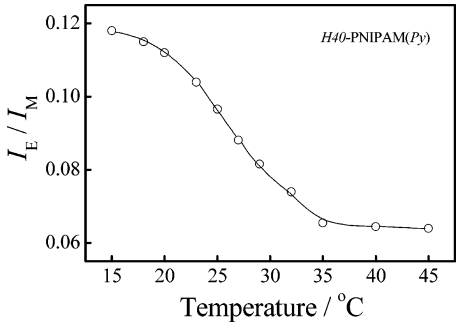

Figure 8. Variation of excimer-to-monomer intensity ratio, I_E/I_M, as a function of temperature for H40−PNIPAM(Py) in aqueous solution at a concentration of 1.0×10^{-3} g/mL.

cycle. The plot of $\langle R_g \rangle / \langle R_h \rangle$ vs temperature in the cooling process exhibits a small dip at ∼32 °C, the minimum value of $\langle R_g \rangle / \langle R_h \rangle$ is ∼0.74. At ∼15 °C, water behaves as a good solvent for the PNIPAM brush, and $\langle R_g \rangle$, $\langle R_h \rangle$, and $\langle R_g \rangle / \langle R_h \rangle$ all converge to similar values for both the heating and cooling cycles.

From Figure 4, we also know that $\langle R_g \rangle$ decreases ∼3 times upon heating. We have previously reported that a decrease of $\langle R_g \rangle$ with a factor of 7 can be observed for free PNIPAM hompolymer chains in aqueous solution.[76] It is possible that densely grafted PNIPAM brush resists fully collapsing, PNIPAM chains are prevented to reach the fully collapsed globule state due to chain crowding and steric repulsion of neighboring PNIPAM chains in the brush. This is also in agreement with theoretical predications.[52]

Microdifferential Scanning Calorimetry (Micro-DSC). To further support and justify our discussion about the double phase transition behavior of densely grafted PNIPAM brush at the surface of hydrophobic H40, we measured the partial heat capacity (C_p) of H40−PNIPAM and H40−PNIPAM(Py) in aqueous solution using a microcalorimeter. Figure 6 shows the temperature dependence of partial heat capacity (C_p) of aqueous solutions of H40−PNIPAM and H40−PNIPAM(Py) at a concentration of 1.0×10^{-3} g/mL, where the heating rate is 1.0 °C/min. For H40−PNIPAM, the micro-DSC curve shows two endothermic peaks located at ∼26 °C and ∼33 °C, respectively. This is the strongest evidence of the existence of double phase transitions for PNIPAM brush at the surface of the dendritic core. The same observation was reported by Tenhu et al.[42] for PNIPAM brush-stabilized gold nanoparticles. The first endothermic peak is relatively broad, while the second peak is quite sharp; the peak temperature of the second transition is close to free PNIPAM chains. For H40−PNIPAM(Py), there also exists two endothermic peaks, with the first broad one located at around 26 °C and the second narrower one located at around 31 °C. The decrease of the second endothermic peak temperature for H40−PNIPAM(Py) as compared to that of H40−PNIPAM can be ascribed to the incorporation of hydrophobic pyrene units into grafted chain.

Fluorescence Measurements. It has been known that pyrene form a cofacial excimer when two pyrene molecules are close (<4 Å) and excited by a light of ∼330 nm.[77] The pyrene excimer shows characteristic fluorescence distinct from an isolated pyrene molecule. The excimer is only stable in its excited state and affected by the collision of its adjacent pyrene molecules. Therefore, the pyrene excimer band at 480 nm is usually accompanied by monomer fluorescence at 380 and 400 nm. Pyrene excimer fluorescence has been successfully used as a probe of helix−helix proximity and protein conformational changes, depending on the ability of two pyrene molecules coming together, which is influenced by the chain mobility and the local concentration of pyrene.[77−82]

Excimer fluorescence measured by the excimer-to-monomer ratio (I_E/I_M) provides highly localized information because the excimer is only formed when aromatic rings closely approach each other.[77] Here, we first labeled the PNIPAM shell with pyrene groups. The fluorescence emission spectra of aqueous H40−PNIPAM(Py) at different temperatures are shown in Figure 7. Besides the monomer bands that are characteristic of the pyrene vibronic structure, which exhibit three distinct peaks at 373, 393, and 415 nm, the excimer emission of pyrene appears as a broad, structureless band around 480 nm. The spectral parameter of interest to us is the excimer (480 nm) to monomer (373 nm) intensity ratio (I_E/I_M).

Figure 8 depicts the temperature dependence of I_E/I_M for H40−PNIPAM(Py) aqueous solution. I_E/I_M decreases continuously with increasing temperature in the range 15−35 °C and keeps almost constant at temperatures above 35 °C. The drop in I_E/I_M should be ascribed to the collapsing of PNIPAM chains in the brush. Upon heating, PNIPAM chains in the densely grafted brush get more hydrophobic, the mobility of chains as well as covalently linked chromophores are increasingly restricted, and they get fewer chances to come close to each other, decreasing the excimer fluorescence intensity relative to the monomer emission. The decrease of I_E/I_M for pyrene-labeled PNIPAM chains upon heating was also observed by Winnik and co-workers.[79] Martinho et al.[80−82] have used equilibrium excimer fluorescence to characterize the coil-to-globule transition, and they always observed a decrease of I_E/I_M accompanying the transition. From excimer fluorescence results, we can tell that PNIPAM chains indeed start to collapse from 15 °C, and the transition is rather broad, spanning from 15 to 35 °C. The obtained fluorescence results do not support the conclusion that the collapsing of the PNIPAM brush is a two-stage process. This should be due to the fact that pyrene groups are randomly

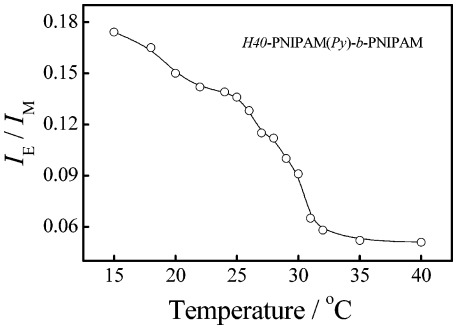

Figure 9. Variation of excimer-to-monomer intensity ratio, I_E/I_M, as a function of temperature for H40−PNIPAM(Py)-*b*-PNIPAM in aqueous solution at a concentration of 1.0×10^{-3} g/mL.

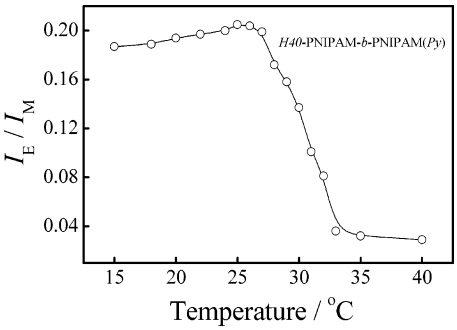

Figure 10. Variation of excimer-to-monomer intensity ratio, I_E/I_M, as a function of temperature for H40−PNIPAM-*b*-PNIPAM(Py) in aqueous solution at a concentration of 1.0×10^{-3} g/mL.

distributed on PNIPAM chains; it cannot differentiate collapsing processes taking place in the inner and outer part of the PNIPAM brush.

We then selectively labeled the inner and outer part of PNIPAM brush with pyrene derivatives, and the prepared samples were denoted H40−PNIPAM(Py)-*b*-PNIPAM and H40−PNIPAM-*b*-PNIPAM(Py), respectively. Excimer fluorescence results are shown in Figures 9 and 10, respectively. When the inner layer of PNIPAM brush was selectively labeled, I_E/I_M of H40−PNIPAM(Py)-*b*-PNIPAM shows gradual decrease in the range 15−32 °C; this is similar to that of H40−PNIPAM-(Py) except that I_E/I_M of H40−PNIPAM(Py) continuously decrease in the range 15−32 °C. This indicates that the collapsing of the inner layer of the PNIPAM brush collapses in a broad temperature range starting from 15 °C. Figure 10 shows the temperature dependences of I_E/I_M of H40−PNIPAM-*b*-PNIPAM(Py), where the outer part of the PNIPAM brush is selectively labeled with pyrene. It is clearly observed that the excimer fluorescence results of H40−PNIPAM-*b*-PNIPAM(Py) is totally different from that of H40−PNIPAM(Py)-*b*-PNIPAM. Upon increasing temperatures, I_E/I_M of H40−PNIPAM-*b*-PNIPAM(Py) first shows a moderate increase in the range 15−27 °C; above that, I_E/I_M gradually decreases in the range 27−33 °C. The initial increase of I_E/I_M should be due to the collapse of the inner unlabeled part of PNIPAM, the contraction of which will render the outer part of PNIPAM segments to be stretched to some extent; this will increase I_E/I_M because pyrene groups from neighboring chains will have larger chances to come close to each. Above 27 °C, the outer part of the PNIPAM brush starts to collapse, leading to decreasing I_E/I_M.

A combination of results from Figures 9 and 10 clearly tells us that the inner part of the PNIPAM brush collapses in the broad temperature range 15−27 °C; above this temperature, the outer part of PNIPAM brush starts to collapse. The excimer fluorescence results of H40−PNIPAM(Py)-*b*-PNIPAM and H40−PNIPAM-*b*-PNIPAM(Py) are generally in agreement with LLS and micro-DSC results, all supporting the double phase transition behavior for the PNIPAM brush at the surface of the H40 core. The collapse of the outer part of PNIPAM above 30 °C is quite understandable; this phase transition can be attributed to the binary segmental interactions changing from repulsive to attractive, just as in the case of free PNIPAM chains in solution above its LCST.[47] The phase transition of the inner part of the PNIPAM brush below 30 °C can be explained using *n*-clusters concepts of de Gennes.[57,59] The inner part of thePNIPAM brush is densely packed, and the collapsing of it at temperatures below 30 °C may also be related to the fact that it is attached to a hydrophobic core. It is well-known when NIPAM monomer are block or randomly copolymerized with a hydrophilic or hydrophobic monomer, its LCST will increase or decrease to some extent.[29] Surely more work is needed to differentiate these two possible explanations. We are currently grafting PNIPAM from a hyperbranched polyglycerol to understand the effect of hydrophilicity of the core on the double phase transition behavior.

Conclusion

Reversible addition-fragmentation transfer (RAFT) polymerization of *N*-isopropylacrylamide (NIPAM) was conducted using a hyperbranched polyester (Boltorn H40) based macroRAFT agent. In aqueous solution, dendritic H40−PNIPAM exists as unimolecular micelles with hydrophobic H40 as the core and grafted PNIPAM chains as the shell. The average grafting density of PNIPAM chains at the H40 core surface is estimated to be 0.46 nm^2 per chain. Experimental results obtained from LLS, micro-DSC, and excimer fluorescence measurements are self-complementary; all of these three techniques unambiguously support the conclusion that PNIPAM brush densely grafted at the surface of hydrophobic dendritic core exhibits double thermal phase transition behavior. The inner part of the PNIPAM brush collapses at lower temperatures (<30 °C); above 30 °C, the outer part of PNIPAM brush starts to collapse. This report provides the first direct evidence of the collapsing sequence of a PNIPAM brush tethered to a spherical hydrophobic core.

Acknowledgment. This work is supported by an Outstanding Youth Fund (50425310) and a key research grant (20534020) from the National Natural Scientific Foundation of China (NNSFC), and the "Bai Ren" project of the Chinese Academy of Sciences.

References and Notes

(1) Hamley, I. W. *The Physics of Block Copolymers*; Oxford University Press: Oxford, 1998; p 131.
(2) Zhang, L. F.; Eisenberg, A. *Science* **1995**, *268*, 1728−1731.
(3) Luo, L. B.; Eisenberg, A. *Langmuir* **2002**, *18*, 1952−1952.
(4) Liu, S. Y.; Billingham, N. C.; Armes, S. P. *Angew. Chem., Int. Ed.* **2001**, *40*, 2328−2331.
(5) Zhang, W. Q.; Shi, L. Q.; Wu, K.; An, Y. L. *Macromolecules* **2005**, *38*, 5743−5747.
(6) Zhang, W. Q.; Shi, L. Q.; An, Y. L.; Gao, L. C.; Wu, K.; Ma, R. J. *Macromolecules* **2004**, *37*, 2551−2555.
(7) Huang, H. Y.; Kowalewski, T.; Remsen, E. E.; Gertzmann, R.; Wooley, K. L. *J. Am. Chem. Soc.* **1997**, *119*, 11653−11659.
(8) Ma, Q. G.; Remsen, E. E.; Kowalewski, T.; Schaefer, J.; Wooley, K. L. *Nano Lett.* **2001**, *1*, 651−655.
(9) Murthy, K. S.; Ma, Q. G.; Remsen, E. E.; Kowalewski, T.; Wooley, K. L. *J. Mater. Chem.* **2003**, *13*, 2785−2795.
(10) Butun, V.; Billingham, N. C.; Armes, S. P. *J. Am. Chem. Soc.* **1998**, *120*, 12135−12136.
(11) Liu, S. Y.; Weaver, J. V. M.; Tang, Y. Q.; Billingham, N. C.; Armes, S. P.; Tribe, K. *Macromolecules* **2002**, *35*, 6121−6131.

(12) Tao, J.; Liu, G. J.; Ding, J. F.; Yang, M. L. *Macromolecules* **1997**, *30*, 4084−4089.
(13) Liu, S. Y.; Weaver, J. V. M.; Save, M.; Armes, S. P. *Langmuir* **2002**, *18*, 8350−8357.
(14) Liu, S. Y.; Armes, S. P. *J. Am. Chem. Soc.* **2001**, *123*, 9910−9911.
(15) Hui, T. R.; Chen, D. Y.; Jiang, M. *Macromolecules* **2005**, *38*, 5834−5837.
(16) Chen, D. Y.; Peng, H. S.; Jiang, M. *Macromolecules* **2003**, *36*, 2576−2578.
(17) Liu, M.; Kono, K.; Frechet, J. M. J. *J. Controlled Release* **2000**, *65*, 121−131.
(18) Aathimanikandan, S. V.; Savariar, E. N.; Thayumanavan, S. *J. Am. Chem. Soc.* **2005**, *127*, 14922−14929.
(19) Zhao, Y. L.; Chen, Y. M.; Chen, C. F.; Xi, F. *Polymer* **2005**, *46*, 5808−5819.
(20) Gillies, E. R.; Frechet, J. M. J. *Drug Discovery Today* **2005**, *10*, 35−43.
(21) Haag, R. *Angew. Chem., Int. Ed.* **2004**, *43*, 278−282.
(22) Thayumanavan, S.; Bharathi, P.; Sivanandan, K.; Vutukuri, D. R. *C. R. Acad. Sci., Ser. IIc: Chim.* **2003**, *6*, 767−778.
(23) Jones, M. C.; Ranger, M.; Leroux, J. C. *Bioconjugate Chem.* **2003**, *14*, 774−781.
(24) Yusa, S.; Sakakibara, A.; Yamamoto, T.; Morishima, Y. *Macromolecules* **2002**, *35*, 10182−10188.
(25) Heise, A.; Hedrick, J. L.; Frank, C. W.; Miller, R. D. *J. Am. Chem. Soc.* **1999**, *121*, 8647−8648.
(26) Hawker, C. J.; Wooley, K. L.; Frechet, J. M. J. *J. Chem. Soc., Perkin Trans. 1* **1993**, 1287−1297.
(27) You, Y. Z.; Hong, C. Y.; Pan, C. Y.; Wang, P. H. *Adv. Mater.* **2004**, *16*, 1953−1957.
(28) Zheng, Q.; Pan, C. Y. *Macromolecules* **2005**, *38*, 6841−6848.
(29) Schild, H. G. *Prog. Polym. Sci.* **1992**, *17*, 163−249.
(30) Stayton, P. S.; Shimoboji, T.; Long, C.; Chilkoti, A.; Chen, G. H.; Harris, J. M.; Hoffman, A. S. *Nature* **1995**, *378*, 472−474.
(31) Hoffman, A. S. *Macromol. Symp.* **1995**, *98*, 645−664.
(32) Park, Y. S.; Ito, Y.; Imanishi, Y. *Langmuir* **1998**, *14*, 910−914.
(33) Okano, T.; Yamada, N.; Okuhara, M.; Sakai, H.; Sakurai, Y. *Biomaterials* **1995**, *16*, 297−303.
(34) Yamada, N.; Okano, T.; Sakai, H.; Karikusa, F.; Sawasaki, Y.; Sakurai, Y. *Makromol. Chem., Rapid Commun.* **1990**, *11*, 571−576.
(35) Kawaguchi, H.; Fujimoto, K.; Mizuhara, Y. *Colloid Polym. Sci.* **1992**, *270*, 53−57.
(36) Luzinov, I.; Minko, S.; Tsukruk, V. V. *Prog. Polym. Sci.* **2004**, *29*, 635−698.
(37) Balamurugan, S.; Mendez, S.; Balamurugan, S. S.; O'Brien, M. J.; Lopez, G. P. *Langmuir* **2003**, *19*, 2545−2549.
(38) Yim, H.; Kent, M. S.; Huber, D. L.; Satija, S.; Majewski, J.; Smith, G. S. *Macromolecules* **2003**, *36*, 5244−5251.
(39) Yim, H.; Kent, M. S.; Mendez, S.; Balamurugan, S. S.; Balamurugan, S.; Lopez, G. P.; Satija, S. *Macromolecules* **2004**, *37*, 1994−1997.
(40) Karim, A.; Satija, S. K.; Douglas, J. F.; Ankner, J. F.; Fetters, L. J. *Phys. Rev. Lett.* **1994**, *73*, 3407−3410.
(41) Nuopponen, M.; Ojala, J.; Tenhu, H. *Polymer* **2004**, *45*, 3643−3650.
(42) Shan, J.; Chen, J.; Nuopponen, M.; Tenhu, H. *Langmuir* **2004**, *20*, 4671−4676.
(43) Turner, K.; Zhu, P. W.; Napper, D. H. *Colloid Polym. Sci.* **1996**, *274*, 622−627.
(44) Zhu, P. W.; Napper, D. H. *J. Colloid Interface Sci.* **1994**, *164*, 489−494.
(45) Zhu, P. W.; Napper, D. H. *Colloids Surf., A* **1996**, *113*, 145−153.
(46) Zhu, P. W.; Napper, D. H. *J. Colloid Interface Sci.* **1996**, *177*, 343−352.
(47) Mattice, W. L.; Misra, S.; Napper, D. H. *Europhys. Lett.* **1994**, *28*, 603−608.
(48) Napper, D. H. *Macromol. Symp.* **1995**, *98*, 911−915.
(49) Hu, T. J.; You, Y. Z.; Pan, C. Y.; Wu, C. *J. Phys. Chem. B* **2002**, *106*, 6659−6662.
(50) Hu, T. J.; Gao, J.; Wu, C. *J. Macromol. Sci., Phys.* **2000**, *B39*, 407−414.
(51) Kidoaki, S.; Ohya, S.; Nakayama, Y.; Matsuda, T. *Langmuir* **2001**, *17*, 2402−2407.
(52) Halperin, A.; Tirrell, M.; Lodge, T. P. *Adv. Polym. Sci.* **1992**, *100*, 31−71.
(53) Zhao, B.; Brittain, W. J. *Prog. Polym. Sci.* **2000**, *25*, 677−710.
(54) Binkert, T.; Oberreich, J.; Meewes, M.; Nyffenegger, R.; Ricka, J. *Macromolecules* **1991**, *24*, 5806−5810.
(55) Szleifer, I.; Carignano, M. A. *Adv. Chem. Phys.* **1996**, *94*, 165−260.
(56) Zhulina, E. B.; Borisov, O. V.; Pryamitsyn, V. A.; Birshtein, T. M. *Macromolecules* **1991**, *24*, 140−149.
(57) Wagner, M.; Brochardwyart, F.; Hervet, H.; Degennes, P. G. *Colloid Polym. Sci.* **1993**, *271*, 621−628.
(58) Teraoka, I. *Polymer Solutions: An Introduction to Physical Properties*; John Wiley & Sons: New York, 2002.
(59) Degennes, P. G. *C. R. Acad. Sci., Ser. IIc: Chim* **1991**, *313*, 1117−1122.
(60) Yang, C.; Li, W.; Wu, C. *J. Phys. Chem. B* **2004**, *108*, 11866−11870.
(61) Frechet, J. M. J. *J. Polym. Sci., Part A: Polym. Chem.* **2003**, *41*, 3713−3725.
(62) Ornatska, M.; Peleshanko, S.; Rybak, B.; Holzmueller, J.; Tsukruk, V. V. *Adv. Mater.* **2004**, *16*, 2206−2209.
(63) Ornatska, M.; Peleshanko, S.; Genson, K. L.; Rybak, B.; Bergman, K. N.; Tsukruk, V. V. *J. Am. Chem. Soc.* **2004**, *126*, 9675−9684.
(64) Ornatska, M.; Bergman, K. N.; Rybak, B.; Peleshanko, E.; Tsukruk, V. V. *Angew. Chem., Int. Ed.* **2004**, *43*, 5246−5249.
(65) Zagar, E.; Zigon, M.; Podzimek, S. *Polymer* **2006**, *47*, 166−175.
(66) Zagar, E.; Zigon, M. *J. Chromatogr., A* **2004**, *1034*, 77−83.
(67) Zagar, E.; Zigon, M. *Macromolecules* **2002**, *35*, 9913−9925.
(68) Xu, J.; Luo, S.; Shi, W.; Liu, S. *Langmuir* **2006**, *22*, 989−997.
(69) Sehgal, R. K.; Kumar, S. *Org. Prep. Proced. Int.* **1989**, *21*, 223−226.
(70) Wu, C.; Xia, K. Q. *Rev. Sci. Instrum.* **1994**, *65*, 587−590.
(71) Gao, J.; Wu, C. *Macromolecules* **1997**, *30*, 6873−6876.
(72) Zhai, X.; Peleshanko, S.; Klimenko, N. S.; Genson, K. L.; Vaknin, D.; Vortman, M. Y.; Shevchenko, V. V.; Tsukruk, V. V. *Macromolecules* **2003**, *36*, 3101−3110.
(73) Tsukruk, V. V.; Shulha, H.; Zhai, X. W. *Appl. Phys. Lett.* **2003**, *82*, 907−909.
(74) Shulha, H.; Zhai, X. W.; Tsukruk, V. V. *Macromolecules* **2003**, *36*, 2825−2831.
(75) Sidorenko, A.; Zhai, X. W.; Peleshanko, S.; Greco, A.; Shevchenko, V. V.; Tsukruk, V. V. *Langmuir* **2001**, *17*, 5924−5931.
(76) Wu, C.; Zhou, S. Q. *Phys. Rev. Lett.* **1996**, *77*, 3053−3055.
(77) Birks, J. B. *Photophysics of Aromatic Molecules*; Wiley: New York, 1970.
(78) Xu, J.; Zhu, Z. Y.; Luo, S. Z.; Wu, C.; Liu, S. Y. *Phys. Rev. Lett.* **2006**, *96*, 027802.
(79) Winnik, F. M. *Macromolecules* **1990**, *23*, 233−242.
(80) Picarra, S.; Relogio, P.; Afonso, C. A. M.; Martinho, J. M. G.; Farinha, J. P. S. *Macromolecules* **2003**, *36*, 8119−8129.
(81) Picarra, S.; Duhamel, J.; Fedorov, A.; Martinho, J. M. G. *J. Phys. Chem. B* **2004**, *108*, 12009−12015.
(82) Picarra, S.; Relogio, P.; Afonso, C. A. M.; Martinho, J. M. G.; Farinha, J. P. S. *Macromolecules* **2004**, *37*, 1670−1670.